Ecological Indicators 11 (2011) 1160–1170

Contents lists available at ScienceDirect

Ecological Indicators

journal homepage: www.elsevier.com/locate/ecolind

Using a sub-pixel mapping model to improve the accuracy of landscape pattern indices

Xiaodong Li, Yun Du, Feng Ling*, Shengjun Wu, Qi Feng

Institute of Geodesy and Geophysics, Chinese Academy of Sciences, 340 Xudong Road, Wuhan, 430077, Hubei, China

ARTICLE INFO

Article history:
Received 6 March 2010
Received in revised form
13 December 2010
Accepted 23 December 2010

Keywords:
Landscape spatial pattern
Landscape pattern index
Sub-pixel mapping
Remotely sensed data
Mixed pixel
Grain size

ABSTRACT

The assessment of landscape spatial patterns is a key issue in landscape management. Landscape pattern indices (LPIs) are tools appropriate for analyzing landscape spatial patterns. LPIs are often derived from raster land cover maps that are extracted from remotely sensed data through hard classification. However, pixel-based hard classification methods suffer from the mixed pixel problem (in which pixels contain more than one land cover class), making for inaccurate classification maps and LPIs. In addition, LPIs generated by hard classification methods are characterized by grain sizes (the sampling unit sizes) that limit the derived landscape pattern to a certain scale. Sub-pixel mapping (SPM) models can enable fine-scale estimation of the spatial patterns of land cover classes without requiring additional data; hence, this is an appropriate downscaling method for land cover mapping. The fraction images generated by soft classification estimate the area proportion of each land cover class within each pixel, and using these images as input enables SPM models to alleviate the mixed pixel problem. At the same time, by transforming fraction images into a finer-scaled hard classification map, SPM models can minimize the influence of grain size on LPIs calculation. In this research, simulated landscape thematic patterns that can provide different landscape spatial patterns, eight commonly used LPIs and a SPM model that maximizes the spatial dependence between neighbouring sub-pixels were applied to assess the efficiency of deriving LPIs from sub-pixel model maps. Results showed that the SPM model can more precisely characterize landscape patterns than hard classification methods can. Landscape fragmentation, class abundance, the uncertainty in SPM, and the spatial resolution of the remotely sensed data influenced LPIs derived from sub-pixel maps. The largest patch index, landscape division, and patch cohesion derived from remotely sensed data with different spatial resolutions through the SPM model were suitable for inter-comparison, whereas the patch density, mean patch area, edge density, landscape shape index, and area-weighted mean shape index derived from the sub-pixel maps were sensitive to the spatial resolution of the remotely sensed data.

1. Introduction

Landscape patterns are formed by a mixture of natural and human-managed patches that vary in size, shape, and arrangement in space; the patterns are also correlated with landscape-scale ecological processes (Turner, 1990; Hulshoff, 1995). Landscape pattern analysis has drawn the attention of researchers because spatial patterns can constrain, promote, or neutralize ecological processes (Li and Wu, 2004). Landscape pattern indices (LPIs) have become increasingly popular to calculate and represent different aspects of landscape spatial patterns (Wu et al., 2002; Li and Wu, 2004). LPIs have become common tools and are viewed as effective for landscape pattern assessment and management; hence, they are important indicators in landscape ecology (Lausch and Herzog, 2002; Schindler et al., 2008; Peng et al., 2010).

LPIs are commonly calculated from categorical maps, which are often raster format land cover maps extracted from remotely sensed data. Numerous classification algorithms have been developed to generate land cover maps from remotely sensed data; traditional classification methods, such as pixel-based supervised classification and pixel-based unsupervised classification, are the most popular methods. Although these methods have been widely used as bases for calculating LPIs, hard classification suffers from critical drawbacks. In hard classification, each pixel is classified into one of many land cover classes, suggesting that land cover exactly fits within the bounds of one or multiple pixels. However, a sizeable proportion of pixels may be a mixture of multiple land cover classes. Within an instantaneous field-of-view, the observed digi-

* Corresponding author. Tel.: +86 27 68881901; fax: +86 27 68881362.
E-mail address: lingf@whigg.ac.cn (F. Ling).

1470-160X/$ – see front matter © 2010 Elsevier Ltd. All rights reserved.
doi:10.1016/j.ecolind.2010.12.016

tal number values of the remotely sensed imagery are always the integration of the radiance from multiple land cover classes, and the spectral mixing within single pixels results in the mixed pixel problem. Consequently, the mixed pixel problem leads to low classification accuracy (Fisher, 1997; Cracknell, 1998; Foody, 2002). Hard classification is a pixel-based classification method, in which mixed pixels are ignored; misclassification of land cover classes due to hard classification consequently yields errors in calculating LPIs (Langford et al., 2006; Shao and Wu, 2008).

Meanwhile, LPIs estimation is influenced by the grain size that is used to quantify the LPIs. LPIs are dependent on the grain size (the sampling unit size) of the categorical map for the raster model, i.e., the grain size of the raster format land cover maps extracted from remotely sensed data (Uuemaa et al., 2005; Bailey et al., 2007). In the creation of land cover maps, smaller grain-sized land cover data are usually preferred for landscape analysis; this is because increasing grain size always leads to the simplification of landscape configuration and decrement in the degree of spatial detail (Zheng et al., 2008). The grain size of hard classification maps is dependent on the spatial resolution of the remotely sensed data. The spatial resolution is determined by the scale of observation (i.e., platforms and sensor types of remotely sensed data). LPIs derived from hard classification maps can represent landscape patterns only at a certain scale because the coarser spatial resolution of the remotely sensed data disregards detailed spatial pattern information on land cover classes. This drawback limits the use of hard classification maps in the derivation of LPIs.

Only a few studies have attempted to solve the mixed pixel problem and minimize the influence of grain size while deriving LPIs. Arnot et al. (2004) applied fuzzy c-means classifier to divide the original image into fuzzy sets so that every location does not fall into a specific land cover class, while allowing each location to belong, to a certain extent, to the two land cover classes within the image. However, fuzzy sets were converted to Boolean classification (hard classification) by identifying the class on the basis of the maximum fuzzy membership within any pixel. This pixel-based classification image suffered from coarse grain size and could not completely represent the spatial patterns of landscapes at the sub-pixel scale. Scaling functions are used to describe variations in LPIs with spatial resolution, thereby showing their potential in downscaling LPIs to minimize the influence of grain size. Saura and Castro (2007) used scaling functions to predict LPIs at the sub-pixel scale. Nevertheless, scaling functions could neither precisely downscale LPIs nor provide sub-pixel land cover spatial patterns. Statistical methods for downscaling land cover maps can provide land cover spatial patterns at a finer scale (Gardner et al., 2008). Instead of remotely sensed data, however, the input used was a raster format land cover map. Furthermore, the influence of the mixed pixel problem over the original input land cover maps was not considered.

As a solution to the mixed pixel problem, soft classification can produce a set of fraction images that predict the area proportion of each land cover class within each pixel. Although the representation of land cover classes generated by this method is more informative and appropriate than that produced by hard classification, directly applying it in calculating LPIs is difficult because no indication of how such classes are distributed spatially within each pixel can be provided (Atkinson et al., 1997; Keshava and Mustard, 2002). With sub-pixel mapping (SPM) models, however, fraction images generated by soft classification can be transformed into a finer-scaled hard classification map that provides the spatial distribution of land cover classes within each coarse pixel. Thus, SPM models that generate finer scaled land cover maps have potential for improving the accuracy of LPIs.

This study aims to derive LPIs from land cover maps that were generated by a SPM model. We intend to provide insights into the following questions: Can the SPM model improve the accuracy of LPIs? What are the main factors influencing the LPIs derived from the sub-pixel maps at the sub-pixel scale?

2. Materials and methods

2.1. Simulated data

The modified random clusters (MRC) simulation method (Saura and Martínez-Millán, 2000; Li and Wu, 2004; Shen et al., 2004) was applied in this study to simulate various landscape patterns using SIMMAP. We considered a simple binary (yes/no) classification of a landscape (e.g., forest/non-forest) into a habitat or non-habitat category and generated resulting binary images. MRC can simulate a wide range of spatial patterns, in which landscape fragmentation and class abundance can be varied (Saura and Martínez-Millán, 2000). Parameter p in a MRC simulation controls the fragmentation of the landscape. Higher values of p (up to an upper limit of $p_c \cong 0.593$) yield larger-sized and fewer patches; thus, the landscape pattern is more aggregated (less fragmented). The lowest value of p that we used in the landscape simulation was $p = 0.4$ because degrees of fragmentation of $p < 0.4$ are not commonly found in most landscapes. The increase in spatial aggregation as a function of p is nonlinear but more rapid near p_c. The proportion of the area occupied by class 1 (A_1, $A_2 = 100 - A_1$) was varied from 10% to 90% in increments of 10% to cover a wide range of landscape configuration possibilities; p was assigned values of 0.4, 0.45, 0.5, 0.525, 0.55, and 0.575, producing 54 different spatial configurations (300×300 pixels for each simulated image). The four-neighbourhood criterion was used in the simulation process (Saura and Martínez-Millán, 2000).

Majority rules were applied to coarsen the images so that remotely sensed data with different spatial resolutions were represented. Majority rules can produce aggregated patterns similar to those obtained by remote sensors with coarser spatial resolutions (Wu et al., 2002; Saura, 2004; Wu, 2004). The "degraded" image pixels were assigned as the most frequent class in the windows of $F \times F$ pixels, where F is the aggregation factor. Eight spatial resolutions that correspond to the aggregation factors, namely, $F = 2, 3, 4, 5, 6, 10, 12$, and 15 pixels, were used in this research. The degraded images also represent classification maps, generated through hard classification methods, of different spatial resolutions. Examples of the resultant patterns for $F = 5$ and $F = 10$ are shown in Fig. 1.

2.2. SPM model

SPM models can be divided into two main groups in terms of goals. The first group considers the spatial dependence of land cover classes, which indicates that sub-pixels that are closer together are more likely to have the same class type than those that are further apart. This SPM model aims to maximize the spatial dependence between neighbouring sub-pixels (Atkinson et al., 1997; Atkinson, 2005; Tatem et al., 2001; Verhoeye and De Wulf, 2002; Mertens et al., 2003; Ling et al., 2008). The second group necessitates ancillary data to provide some priori spatial models at a finer scale. With the spatial pattern information retrieved from ancillary training data (e.g., aerial photographs), this SPM model aims to generate spatial patterns of land cover classes at the sub-pixel scale that share characteristics with the spatial patterns in the training data (Tatem et al., 2002; Boucher et al., 2008; Boucher, 2009). Various algorithms such as the Hopfield neural network (HNN) (Tatem et al., 2001; Tatem et al., 2002), pixel swapping (Atkinson, 2005; Makido et al., 2007), and Markov random field (Kasetkasem et al., 2005; Tolpekin and Stein, 2009) have been proposed for use in SPM models in both groups mentioned above.

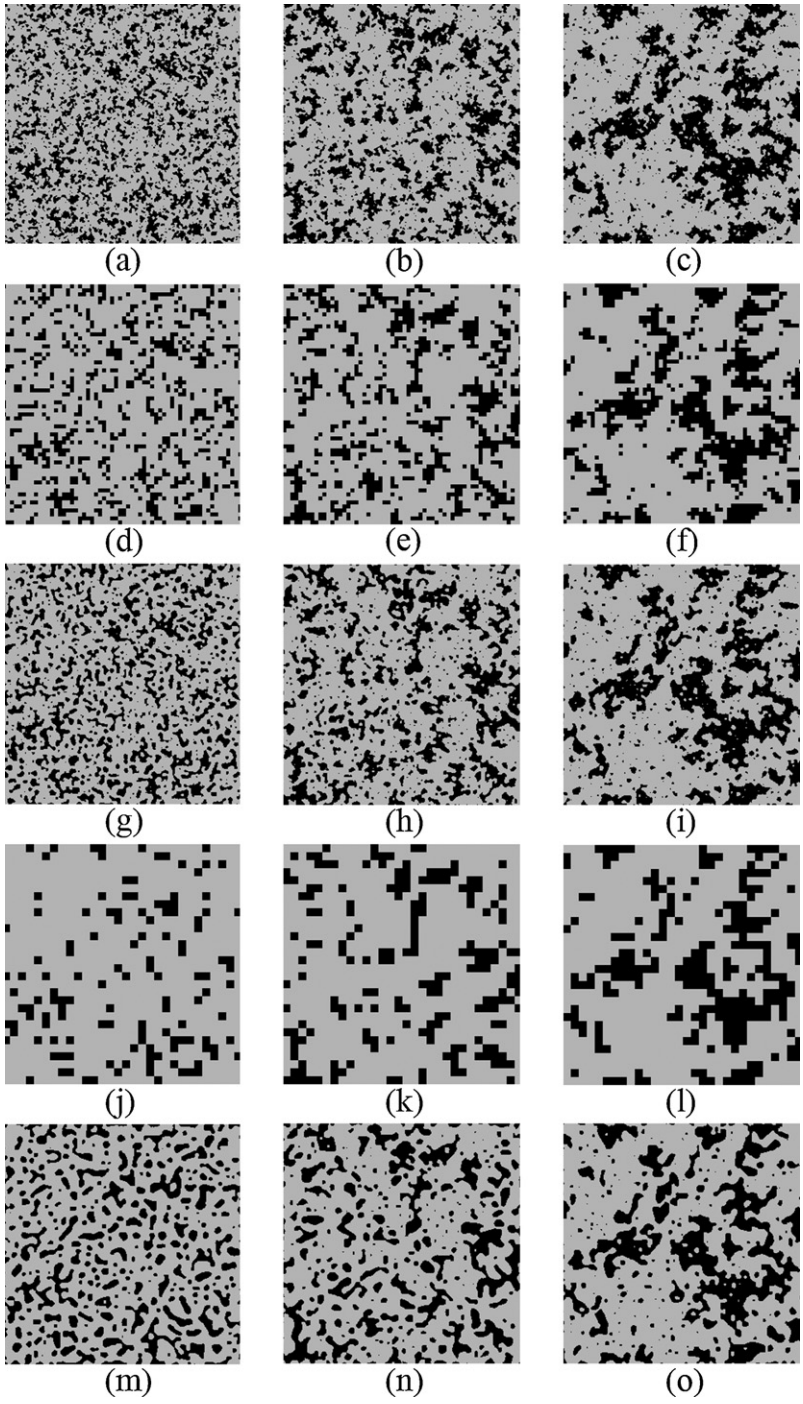

Fig. 1. (a), (b), and (c) are simulated images for $A_1 = 30\%$ (A_1 represents class abundance of the focal class) and $p = 0.4$, 0.5, and 0.55, respectively (p is the parameter that controls landscape fragmentation, and higher values of p yield more aggregated landscape pattern); (d), (e), and (f) represent a lower level of spatial resolution with aggregation factor $F = 5$ for the hard classification maps, and (g), (h), and (i) are the corresponding sub-pixel maps; (j), (k), and (l) represent a higher level of spatial resolution with aggregation factor $F = 10$ for the hard classification maps, and (m), (n), and (o) are the corresponding sub-pixel maps. Black is the focal land cover class and grey pertains to the other land cover classes.

Only the first SPM model was considered in this research to avoid the need for ancillary data, which are not easily acquired in practice. The pixel-swapping algorithm (Atkinson, 2005) was applied in the model. With this algorithm, the class proportions in the coarse resolution pixels (pixels of remotely sensed data) remain identical before and after SPM; in addition, this algorithm is considered a relatively efficient method in terms of accuracy and computation time (Makido et al., 2007; Atkinson, 2009). In the initializing step of the pixel-swapping algorithm, the sub-pixels that represent different land cover classes are randomly allocated within each coarse pixel based on the class proportions extracted from soft classification. Only binary maps were considered in this research; hence, the sub-pixel is assigned the values "0" or "1", representing the two land cover classes (non-habitat and habitat). Then, the sub-pixels are swapped iteratively to maximize the spatial dependence between neighbouring sub-pixels based on the distance weighted function (attractiveness, A_i) of each sub-pixel. The nearest neighbour function that gives equal weight to its near-

est neighbouring sub-pixels is applied. In the nearest neighbour model, attractiveness A_i for sub-pixel X_i is calculated by the sum of the sub-pixels, which have the same land cover class (values "0" or "1") as X_i.

$$A_i = \sum_{j=1}^{n} Z(X_j) \quad (1)$$

where n is the number of neighbours of sub-pixel X_i and $Z(X_j)$ is the value of class Z at the jth pixel location X_j.

Within a coarse pixel, four A_i are computed. $A_i\_0\_bef$ is the minimum A_i value allocated to a "0" in location x and $A_i\_1\_bef$ is the minimum A_i value allocated to a "1" in location y. $A_i\_0\_aft$ is the A_i value for "0" in location y and $A_i\_1\_aft$ is the A_i value for "1" in location x. If the sum of $A_i\_0\_aft$ and $A_i\_1\_aft$ is larger than that of $A_i\_0\_bef$ and $A_i\_1\_bef$, this pair of sub-pixels is swapped. If the coarse pixel contains only one land cover class, then no swapping of sub-pixels is performed. This procedure is iteratively performed until the swapping of sub-pixels can no longer increase the spatial dependence of land cover classes within the entire image.

The sizes of sub-pixels for different degraded images are set equal to the minimum mapped unit of the MRC simulated images, i.e., one pixel of each simulated image that contains 300 × 300 pixels. This approach ensures that each sub-pixel represents only one land cover class. It also enables the assessment of the accuracy of LPIs derivation from remotely sensed data at different levels of spatial resolutions (i.e., different aggregation factors used to coarsen the images). At different coarse spatial resolutions, the contributions of each sub-pixel were added up to obtain a pixel-scale proportion for each land cover class. These pixel-scale proportions are considered the output of soft classification (Makido et al., 2007). Moreover, SPM is an inverse problem that reconstructs a finer-scaled land cover map from a set of class proportions through a coarse-resolution image. However, this inverse problem underdetermines that different fine-scaled land cover maps can match the original coarse-resolution class proportions; uncertainties also exist in the results of fine-scaled land cover maps (Atkinson, 2009; Boucher, 2009). The pixel-swapping algorithm used in this study is a spatial optimization approach. The goal is to maximize the spatial dependence between neighbouring sub-pixels, and the constraint is to match the original pixel proportions generated by the soft classification method. Therefore, the results of the sub-pixel maps that were generated by the pixel-swapping algorithm differ because of the uncertainty in SPM. For each degraded image, we ran the model 50 times to achieve reliable LPIs through SPM.

2.3. Analyzed LPIs

Eight commonly used LPIs, which characterize the composition and configuration of landscapes, were analyzed (Jaeger, 2000; Saura, 2004; Saura and Castro, 2007). Using Fragstats 3.3 (McGarigal et al., 2002), all LPIs were computed at the class level, i.e., only patches that belong to a certain class were considered. The eight LPIs were patch density (PD), mean patch area (MPA), edge density (ED), landscape shape index (LSI), area-weighted mean shape index (AWMSI), largest patch index (LPI), landscape division (LD), and patch cohesion (PC).

3. Results and discussion

3.1. Comparison of LPIs derived from the sub-pixel and hard classification maps

The variations of LPIs with coarse spatial resolution at both the pixel scale (i.e., LPIs derived from the hard classification maps) and the sub-pixel scale (i.e., LPIs derived from the sub-pixel maps) are shown in Figs. 2–4. Compared with the reference landscape pattern of the focal land cover class, the accuracy of LPIs was improved when the SPM model was used; this improvement is attributed to the advantages of the SPM model in terms of solving the mixed pixel problem and minimizing the influence of grain size on the quantification of LPIs. In comparison with hard classification methods, considerable improvements in accuracy were achieved using the SPM model in calculating PD, MPA, ED, LSI, and AWMSI in all cases, as well as LPI, LD, and PC in certain circumstances. The accuracies of the LPIs derived from the sub-pixel maps varied considerably with landscape fragmentation, class abundance, and the spatial resolution of the remotely sensed data. First, more accurate LPIs were derived from the sub-pixel maps in less fragmented landscapes. Second, the derived LPI, LD, and PC were very close to the reference LPIs when the focal class occupied the majority of the landscape area (high class abundance). Conversely, the accuracy of PD, MPA, ED, LSI, and AWMSI did not show this trend. Finally, LPIs were more accurate with finer spatial resolution of the remotely sensed data at both the pixel and sub-pixel scales. For the PD, MPA, ED, LSI, and AWMSI derived from the sub-pixel maps, the accuracy noticeably decreased when the spatial resolution of the remotely sensed data was coarsened. For the LPI, LD, and PC derived from the sub-pixel maps, the variations in accuracy with coarse spatial resolution differed with class abundance. Furthermore, as shown by the error bars in Figs. 2–4, uncertainty existed in the LPIs derived from the sub-pixel maps, and the uncertainty increased most often with coarser spatial resolution. The values of the error bars were small for PD, MPA, ED, LSI, and AWMSI, indicating less uncertainty. For LPI, LD, and PC, the error bar values were relatively large in certain circumstances and varied sharply with landscape fragmentation, class abundance, and coarse spatial resolution.

3.2. Factors that influence LPIs derived from the sub-pixel maps

Although the accuracy of LPIs was improved through the SPM model, the LPIs derived from the sub-pixel maps did not fully represent the reference landscape pattern (Figs. 2–4). The objective function in the SPM model that was used to allocate the sub-pixels, together with the uncertainty in SPM and the resultant land cover maps, landscape fragmentation, class abundance, and the spatial resolution of the remotely sensed data all influenced the LPIs derived from the sub-pixel maps.

3.2.1. SPM model and the uncertainty in SPM

The limitation of the LPIs derived from the sub-pixel maps in representing the actual landscape pattern is attributed mainly to the objective function of the SPM model. Maximizing land cover spatial dependence in the objective function assumes that sub-pixels that are close together are more likely to have the same land cover class type. However, this principle can hardly represent various real-world landscape patterns. For the pixel-swapping algorithm, the objective function determines the spatial allocation of sub-pixels, and only the swapping of sub-pixels, which increases spatial dependence, is performed in the optimization approach. Therefore, in the resultant sub-pixel maps, sub-pixels representing the same land cover class are aggregated into one or a few patches within each coarse pixel, or aggregated with the sub-pixels of neighbouring coarse spatial resolution pixels. This approach implies that isolated sub-pixels of a land cover class seldom exist within the coarse spatial resolution pixels. This aggregation of sub-pixels eliminated small-sized patches, which were substituted with larger aggregated patches (Fig. 1). As a result, the SPM model decreased the degree of landscape fragmentation by generating more aggregated landscapes, and the landscape pattern yielded by the SPM model was not consistent with the reference pattern. For PD, ED, LSI, AWMSI, and LD, for which lower values indicate more aggregated landscapes, the values of the LPIs derived from the sub-

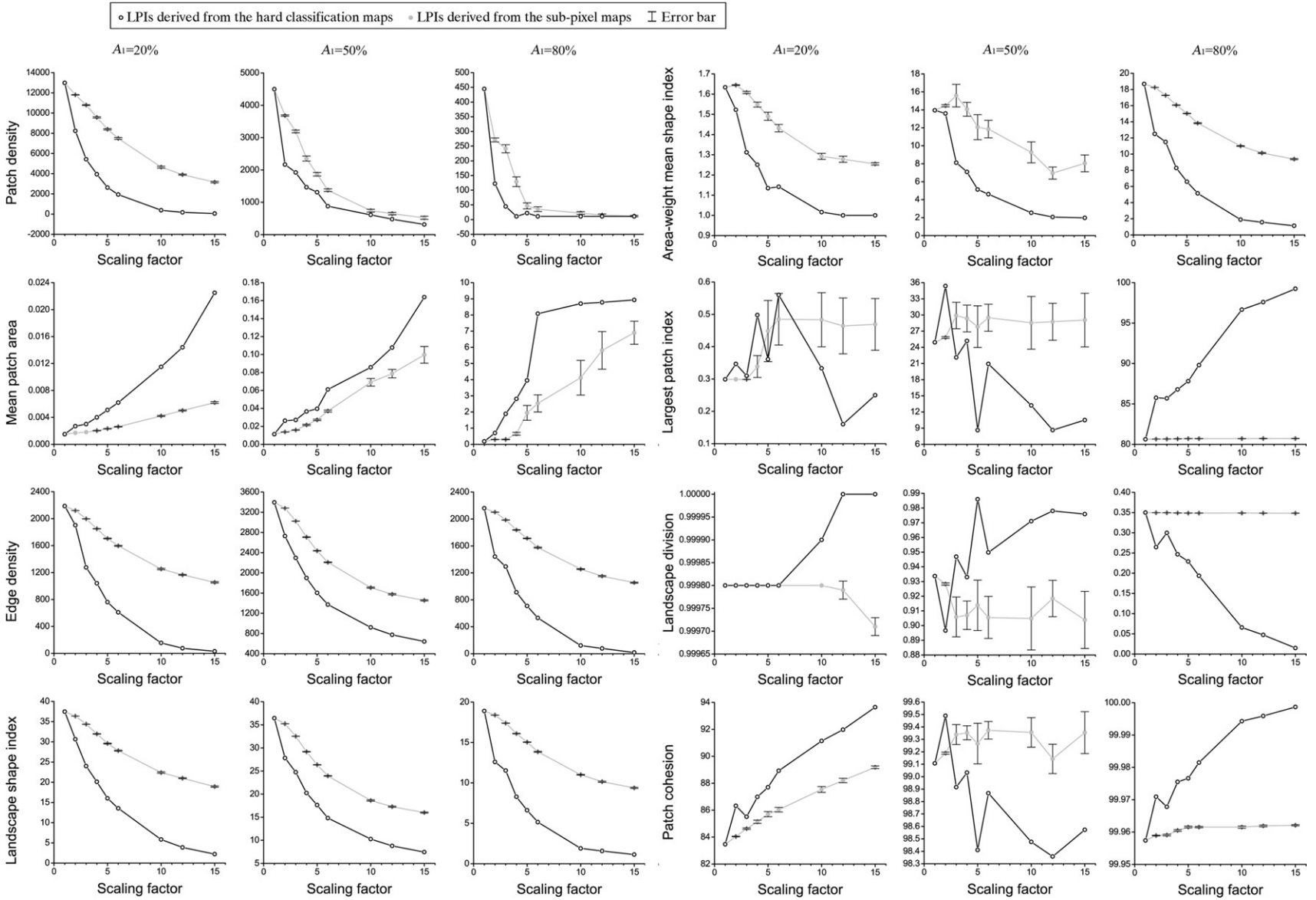

Fig. 2. Comparison of the class-level LPIs derived from the sub-pixel and hard classification maps. The behaviour of LPIs as a function of the coarse spatial resolution (scaling factor) for $p = 0.4$, and $A_1 = 20\%$, 50%, and 80%. LPIs with scaling factor = 1 represent the reference landscape pattern of the focal land cover class. Each error bar represents mean ± SD.

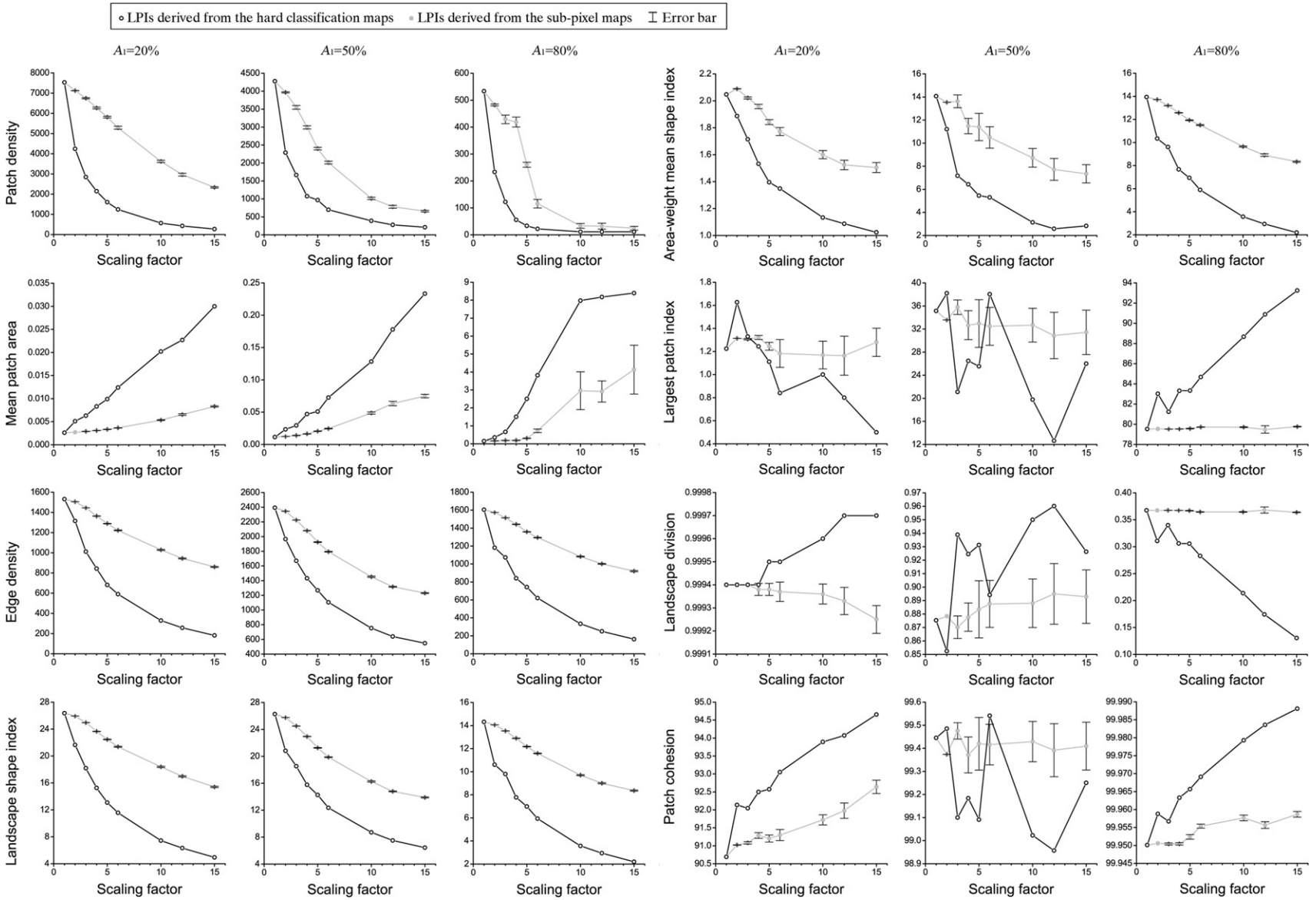

Fig. 3. Comparison of the class-level LPIs derived from the sub-pixel and hard classification maps. The behaviour of LPIs as a function of the coarse spatial resolution (scaling factor) for $p = 0.5$, and $A_1 = 20\%$, 50%, and 80%. LPIs with scaling factor = 1 represent the reference landscape pattern of the focal land cover class. Each error bar represents mean ± SD.

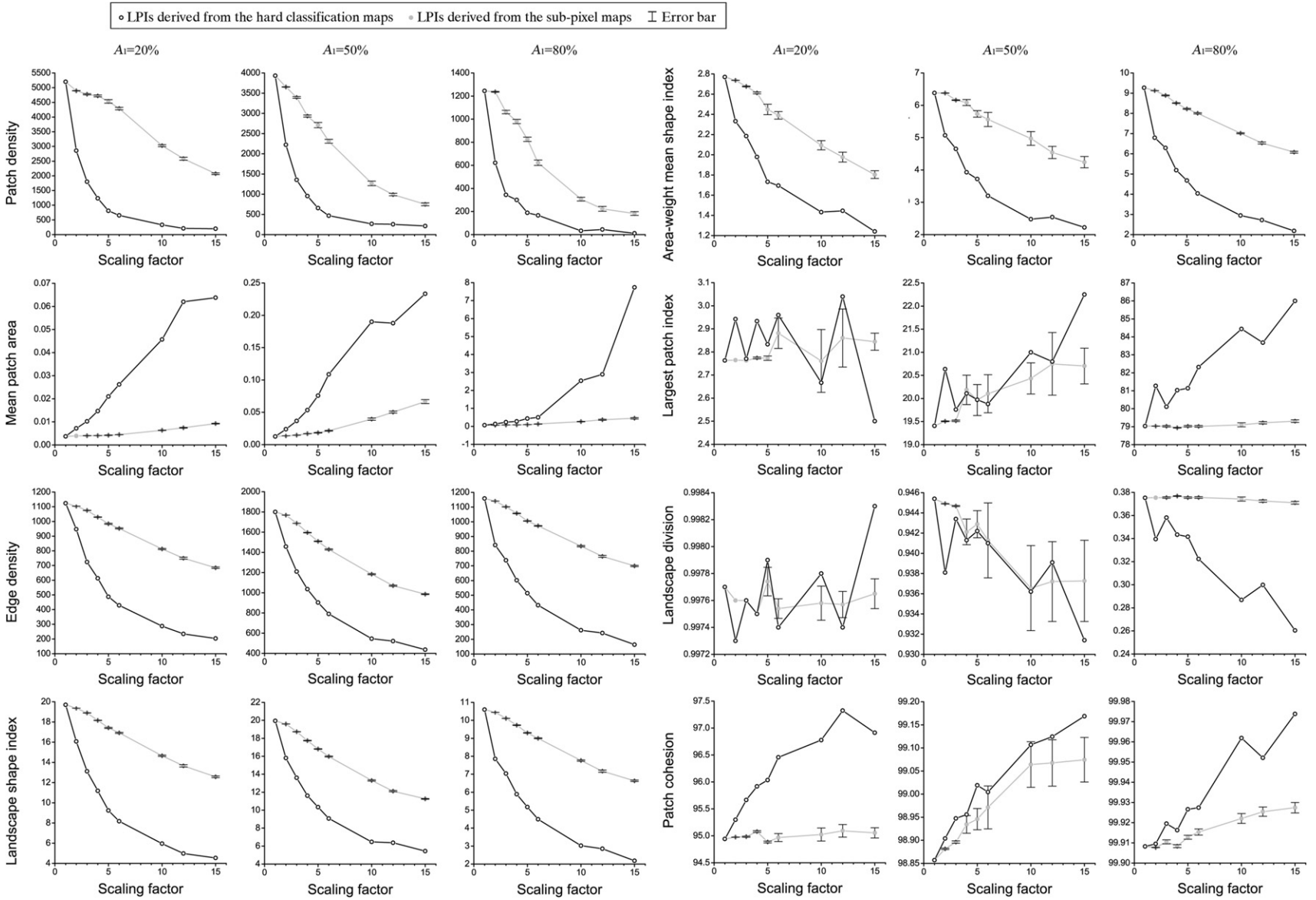

Fig. 4. Comparison of the class-level LPIs derived from the sub-pixel and hard classification maps. The behaviour of LPIs as a function of the coarse spatial resolution (scaling factor) for $p = 0.55$, and $A_1 = 20\%$, 50%, and 80%. LPIs with scaling factor = 1 represent the reference landscape pattern of the focal land cover class. Each error bar represents mean ± SD.

pixel maps were lower than those of the reference LPIs. For MPA, LPI, and PC, for which higher values indicate more aggregated landscapes, the values of the LPIs derived from the sub-pixel maps were higher than those of the reference LPIs (Figs. 2–4).

The LPIs derived from the sub-pixel maps were influenced by the uncertainty in SPM. As SPM is an under-determined inverse problem, the resultant sub-pixel maps from different or even the same SPM algorithms are probably not identical, although all satisfy the constraints of the original class proportions by the coarse resolution image (Atkinson, 2009; Boucher, 2009). Because the SPM model is applied to determine the most likely locations of the fractions of each land cover class within each coarse pixel, the initialization step and spatial optimization approach for allocating the sub-pixels in the SPM model result in uncertainty in the sub-pixel maps and resultant LPIs. The uncertainty in the LPIs derived from the sub-pixel maps is exhibited using error bars in Figs. 2–4. Substantial uncertainties in the LPIs were most frequently found with coarser spatial resolution of the remotely sensed data. Generally, for the PD, MPA, ED, LSI, and AWMSI derived from the sub-pixel maps, the uncertainty was low and did not considerably affect their accuracies. Considering the influence of uncertainty, the LPI, LD, and PC derived from the sub-pixel maps for certain class abundances did not show appreciable improvement in accuracy over those derived from hard classification maps. However, the absolute values of the error bars were rather small for these LPIs. Despite its uncertainty, therefore, the SPM model is practicable in generating land cover maps for calculating LPIs from the sub-pixel maps. Moreover, the uncertainty indicates that sufficient repetitions of SPM are needed to obtain reliable LPIs, with greater uncertainty implying more repetitions required.

3.2.2. Landscape fragmentation and class abundance

Landscape fragmentation has been broadly applied in many aspects of ecology, including composition (number/size), shape (perimeter/edge), and configuration (degree of connectedness). The eight LPIs used in this research reflect different aspects of landscape fragmentation. Among these LPIs, PD and MPA directly depict the density in number and mean size of patches; ED, LSI, and AWMSI, which are related to edge, are used to characterize patch shape regularity; LPI is used to characterize domain patch size; and LD and PC are used to characterize configuration. Fragmentation is defined as the process of increasing the number of patches, decreasing mean patch size, and increasing the total amount of edge; thus, the SPM model, which aims to maximize spatial land cover dependence, decreases patch numbers by generating larger-sized and regularly shaped patches. The model consequently decreases the degree of landscape fragmentation compared with the reference landscape. As a result, the accuracies of PD, MPA, ED, LSI, and AWMSI decreased with the decrease in landscape fragmentation caused by the SPM model; hence, the sub-pixel maps could not reach the level of accuracy reflected by the reference landscape pattern (Figs. 2–4). Moreover, the degrees of landscape fragmentation and accuracies of the PD, MPA, ED, LSI, and AWMSI derived from the sub-pixel maps decreased gradually when the spatial resolution of the remotely sensed data was coarsened (Figs. 2–4). The LPI, LD, and PC derived from the sub-pixel maps were also affected by the decrement in landscape fragmentation. However, their values did not vary linearly with the changes in patch number, mean size, and shape regularity, and they exhibited a different trajectory when the spatial resolution of the remotely sensed data was coarsened.

In addition, the decrement in fragmentation of the actual landscapes by the SPM model was more evident in more fragmented landscapes. Therefore, the classification accuracy of the SPM model and accuracy of LPIs derived from the sub-pixel maps were higher in more aggregated landscapes. A visual comparison of the sub-pixel maps of varying fragmentation (Fig. 1) and the subsequent LPIs derived from the sub-pixel maps (Figs. 2–4) shows that the SPM model worked more precisely for more aggregated landscapes.

Class abundance should also be considered when using the SPM model in improving LPIs. With the increment in class abundance, the changes in patch number and area were clearly observable, and fewer and larger area patches of the focal class were generated. These changes are correspondingly reflected in the classification maps (Figs. 2–4). For hard classification, higher class abundance of the focal class enabled the classification of more pixels to that class and often generated larger patches, as well as leading to obvious changes in NP, MPA, and AWMSI. For the SPM model, class abundance affected the number of sub-pixels to be aggregated. More sub-pixels of the focal class were aggregated into larger patches when class abundance was high, and obvious changes in NP, MPA, and AWMSI were also observed in the sub-pixel maps. The other LPIs, which are not used to depict the number and mean size of patches, exhibited no significant changes with the increment in class abundance in both the hard classification and sub-pixel maps.

Moreover, the accuracy of LPIs was not always improved through the SPM model in certain cases of class abundance. PD, MPA, ED, LSI, and AWMSI were all derived more accurately from the sub-pixel maps than from the hard classification maps irrespective of class abundance. For LPI, LD, and PC, however, the SPM model did not show extensive advantage in some class abundances in terms of accuracy and uncertainty (Figs. 2–4). The LPI derived from the sub-pixel maps remained almost invariant to changes in coarse spatial resolution when the corresponding patch type occupied the majority of the landscape. This is because almost all the sub-pixels of the focal class are aggregated despite coarse spatial resolution. The same tendency can be found in LD, which is highly correlated with LPI with high class abundance. PC measures the connectedness of the corresponding patch type. Below a threshold, PC is sensitive to the aggregation of the focal class and increases as the sub-pixels of the focal class are gradually aggregated. Above the threshold, the connectedness is stable and PC becomes robust to the aggregation.

3.2.3. Spatial resolution of the remotely sensed data

The accuracy of and uncertainty in the LPIs derived from the sub-pixel maps were also affected by the spatial resolution of the remotely sensed data, which was represented in this research as the aggregation factor for the degraded images. Remotely sensed data with fine spatial resolution are preferable in deriving landscape patterns at the sub-pixel scale. In SPM, coarser spatial resolution of the remotely sensed data indicates more varied land cover classes involved in each coarse pixel. Nevertheless, sub-pixels can only be allocated within their corresponding coarse pixels, and coarser spatial resolution indicates a larger area of potential locations for sub-pixels to be allocated in the resultant sub-pixel maps. This increases the uncertainty in the sub-pixel maps and decreases the accuracy of the corresponding LPIs. By contrast, finer spatial resolution can reduce the uncertainty in allocating sub-pixels, reducing the number of wrongly allocated sub-pixels and generating more accurate landscape patterns at the sub-pixel scale (Figs. 2–4).

Considering the influencing factors in deriving LPIs from sub-pixel maps, the objective function of the SPM model and uncertainty in the result of the sub-pixel maps are intrinsic factors of SPM. The influence of these factors cannot be eliminated. Landscape fragmentation and class abundance are inherent in the focal study area and cannot be disregarded. However, the spatial resolution of the remotely sensed data can be adjusted using different satellite data. Moreover, with the development and application of remote sensing systems, multi-resolution satellite data have been widely used for regional monitoring, and multi-scale analyses of landscape pattern are crucial for evaluating landscape context (Purtauf et al., 2005). The inter-comparison of LPIs derived

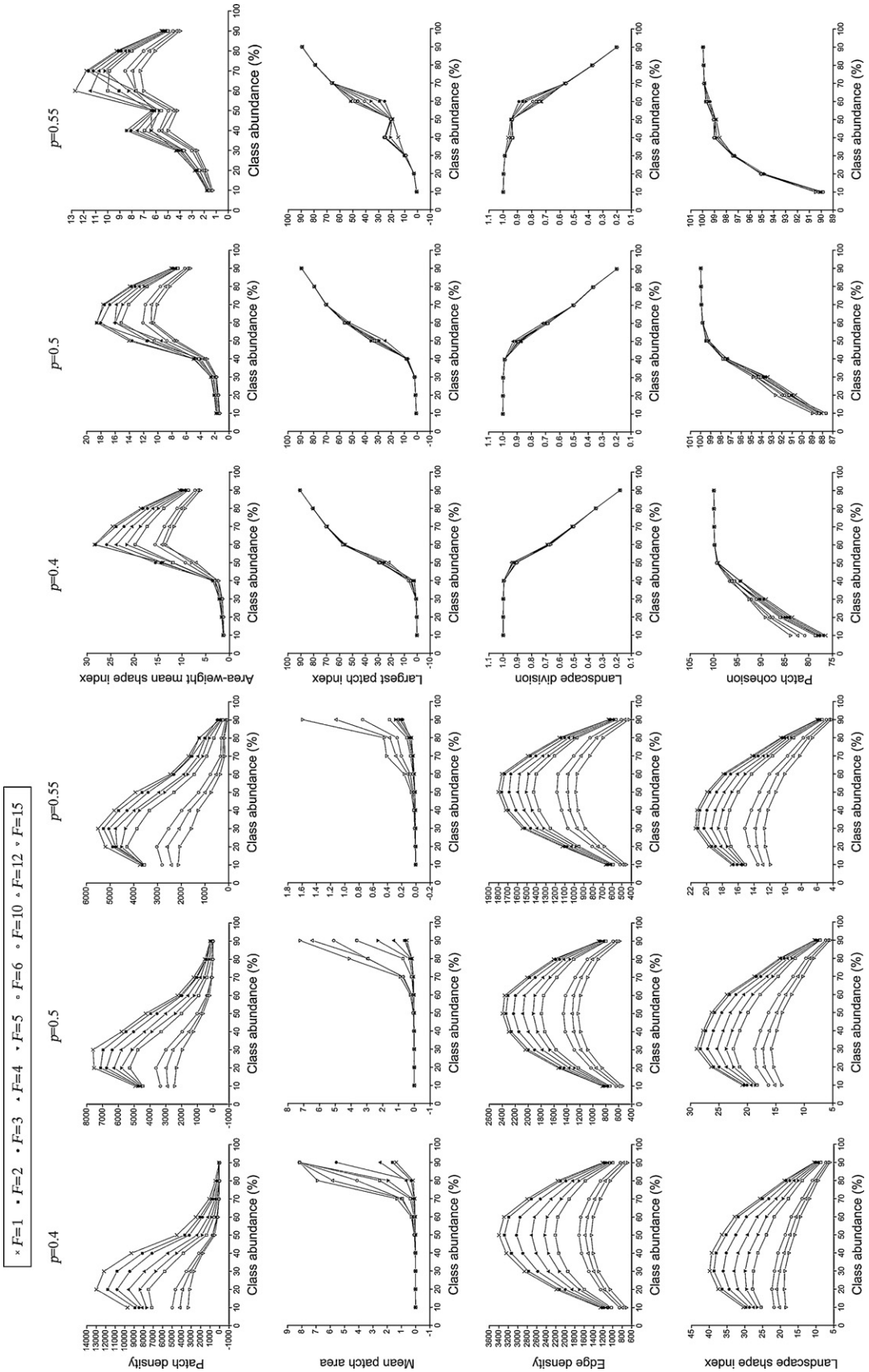

Fig. 5. Behaviour of LPIs with the coarse spatial resolution (i.e., aggregation factor *F*) as a function of class abundance for $p = 0.4$, 0.5, and 0.55.

Table 1
Sensitivity (S) of LPIs derived from the hard classification and sub-pixel maps.

Index	S (for LPIs derived from the hard classification maps)	S (for LPIs derived from the sub-pixel maps)
PD	−106.394	−82.247
MPA	59.370	38.450
ED	−135.852	−91.370
LSI	−137.767	−85.692
AWMSI	−93.478	−43.582
LPI	5.549	1.387
LD	−11.753	−1.015
PC	26.212	6.482

from sub-pixel maps of different spatial resolutions is particularly significant.

The inter-comparison of the LPIs derived from the sub-pixel maps of the same grain size (sub-pixel size) using multi-resolution satellite data is shown in Fig. 5. The sensitivity of the LPIs derived from the sub-pixel maps to changes in coarse spatial resolution (S) is estimated as follows (O'neill et al., 1996):

$$S = 100\frac{M^{10} - M^{3}}{\mathrm{SD}} \quad (2)$$

where M^{x} is the mean value of the landscape pattern index for $F = x$; SD is the standard deviation of LPIs for the set of simulated patterns with all class abundance and $p \geq 0.4$. As noted in the MRC simulation method that generated various landscape patterns used in this research, the degrees of fragmentation were obtained with $p \geq 0.4$ to represent commonly found landscape patterns. Including all p values in the computation of SD would over-estimate the variation range of LPIs (Saura and Martínez-Millán, 2000). S values allow for a more appropriate and adequate comparison of the sensitivity of LPIs. S represents the percentage of the absolute variation of the landscape index to changes in coarse spatial resolution relative to the overall range of variation in the index (as estimated by SD). The nearer S is to 0, the more robust the index is to changes in coarse spatial resolution (from $F = 10$ to $F = 3$). Positive S values indicate that the index tends to increase with coarse spatial resolution, and vice versa. The sensitivities of the LPIs derived from the hard classification and sub-pixel maps to changes in coarse spatial resolution were analyzed in this research. Table 1 shows S values for the eight analyzed LPIs.

For hard classification methods, coarsening the spatial resolution of the remotely sensed data (e.g., from $F = 3$ to $F = 10$ in Table 1) yielded larger-sized, more regularly shaped, and fewer patches, along with more connectivity and less fragmented landscape patterns. For the SPM model, coarser spatial resolution of the remotely sensed data presented more sub-pixels of the same class to be aggregated within the area defined by the coarse spatial resolution. Subsequently, coarsening the spatial resolution of the remotely sensed data resulted in similar changes in landscape patterns in the sub-pixel maps as in the hard classification maps (Table 1). The sign (positive or negative) of S shows that the LPIs derived from both the hard classification and SPM modeled maps had the same trend of variation when spatial resolution was changed. PD, ED, LSI, AWMSI, and LD tended to decrease with coarser spatial resolution, whereas MPA, LPI, and PC tended to increase. The values of S show that the LPIs derived from both the hard classification and sub-pixel maps had similar sensitivity to coarse spatial resolution. LPI, LD, and PC were robust to coarse spatial resolution, whereas the other LPIs, in general, were highly sensitive and unsuitable for inter-comparison across different coarse spatial resolutions. Greater sensitivity was reflected by PD, MPA, ED, LSI and AWMSI, which are used to characterize patch number, mean size, and shape regularity that exhibit significant changes caused by the aggregation of landscapes brought by the SPM model. The accuracies of these sensitive LPIs clearly decreased with the decrement in landscape fragmentation caused by the SPM model, especially from coarser spatial resolution of the remotely sensed data. Consequently, some sensitive LPIs (e.g., PD, ED, LSI, and AWMSI) would be under-estimated and some LPIs (e.g., MPA) would be over-estimated from coarser spatial resolution images at the sub-pixel scale.

4. Conclusions

This research assessed the derivation of LPIs from sub-pixel maps through the SPM model, which aims to maximize the spatial dependence between neighbouring sub-pixels. Using the output of soft classification, the SPM model transforms fraction images into a finer-scaled hard classification map, consequently alleviating the mixed pixel problem and minimizing the influence of grain size on LPIs quantification which the traditional pixel-based hard classification methods typically suffer from. The pixel-swapping algorithm, which can be used without ancillary data and prior information, was employed to generate land cover maps from which LPIs were calculated. Eight LPIs were applied, and the results showed that the LPIs derived from the sub-pixel maps were, in general, preferable to those derived from the hard classification maps in terms of accuracy.

The factors influencing the LPIs derived from the sub-pixel maps were analyzed. First, insufficient expression of land cover spatial pattern in the objective function is the intrinsic factor that limits the SPM model in representing landscape spatial patterns. SPM also generated uncertainty in the derived LPIs. Second, landscape fragmentation and class abundance affected the values and scaling behaviours of the LPIs derived from the sub-pixel maps. Most of the LPIs derived from the sub-pixel maps can be generated more accurately in less fragmented landscapes, and the LPI, LD, and PC derived from the sub-pixel maps can approximate those of the reference landscape patterns when class abundance is high. Finally, finer spatial resolution of the remotely sensed data yielded more accurate and less uncertain LPIs with the SPM model.

The inter-comparison of the LPIs derived from the sub-pixel maps of the same sub-pixel size using multi-resolution satellite data was also addressed. The LPIs derived from the SPM modeled maps exhibited the same trend of variation (increase or decrease) as the LPIs derived from the hard classification maps when the spatial resolution of the remotely sensed data was changed. PD, MPA, ED, LSI, and AWMSI were sensitive to the spatial resolution of the remotely sensed data when derived from land cover maps using the SPM model, and were consequently unsuitable for inter-comparison across different coarse spatial resolutions at the sub-pixel scale. By contrast, LPI, LD, and PC derived from the sub-pixel maps were robust to the spatial resolution of the remotely sensed data.

Although this research has analyzed the impacts of the SPM model on landscape pattern, several other aspects require further study. First, only a binary landscape was considered in this research. Because actual landscapes are composed of a variety of land cover classes, handling multiple land cover classes at the sub-pixel scale is required. Second, we operated under the assumption that the proportions of land cover classes for each pixel have been obtained accurately by soft classification. Nevertheless, the error caused by soft classification will affect SPM, and consequently influence the LPIs to a certain extent. Studies on the uncertainty propagation of soft classification in SPM models and LPIs derived from sub-pixel maps at the sub-pixel scale are significant. Third, the pixel-swapping algorithm that maximizes the spatial dependence between neighbouring sub-pixels was adopted. Other SPM algorithms, however, can offer advantages in improving the accuracy

of LPIs in certain aspects. For example, the HNN algorithm provides proportions of sub-pixels in the resultant sub-pixel map that are not completely consistent with the fraction images of soft classification, an attribute that can potentially reduce uncertainty in sub-pixel maps and resultant LPIs. Comprehensive studies on LPIs derivation from sub-pixel maps through SPM models are required before recommendations can be made as to which method is best for application.

Acknowledgments

This work was supported in part by the Knowledge Innovation Program of the Chinese Academy of Sciences (No. kzcx2-yw-141), the Natural Science Foundation of China (No. 40801186), Wuhan Youth Chenguang Project (No. 200950431218) and National Key Technology R&D Program (2006BAC10B). The authors would like to thank the Santiago Saura Martínez for providing the SIMMAP software and Kevin McGarigal, Eduard Ene and Chris Holmes for providing the Fragstats software used in this study. We are particularly grateful to the anonymous reviewers for their helpful comments on the earlier version of this paper.

References

Arnot, C., Fisher, P., Wadsworth, R., Wellens, J., 2004. Landscape metrics with ecotones: pattern under uncertainty. Landscape Ecol. 19, 181–195.
Atkinson, P., 2005. Sub-pixel target mapping from soft-classified, remotely sensed imagery. Photogramm. Eng. Remote Sens. 71, 839–846.
Atkinson, P., 2009. Issues of uncertainty in super-resolution mapping and their implications for the design of an inter-comparison study. Int. J. Remote Sens. 30, 5293–5308.
Atkinson, P., Cutler, M., Lewis, H., 1997. Mapping sub-pixel proportional land cover with AVHRR imagery. Int. J. Remote Sens. 18, 917–935.
Bailey, D., Herzog, F., Augenstein, I., Aviron, S., Billeter, R., Szerencsits, E., Baudry, J., 2007. Thematic resolution matters: indicators of landscape pattern for European agro-ecosystems. Ecol. Indicators 7, 692–709.
Boucher, A., 2009. Sub-pixel mapping of coarse satellite remote sensing images with stochastic simulations from training images. Math. Geosci. 41, 265–290.
Boucher, A., Kyriakidis, P., Cronkite-Ratcliff, C., 2008. Geostatistical solutions for super-resolution land cover mapping. IEEE Trans. Geosci. Remote Sens. 46, 272–283.
Cracknell, A., 1998. Review article Synergy in remote sensing-what's in a pixel? Int. J. Remote Sens. 19, 2025–2047.
Fisher, P., 1997. The pixel: a snare and a delusion. Int. J. Remote Sens. 18, 679–685.
Foody, G., 2002. Status of land cover classification accuracy assessment. Remote Sens. Environ. 80, 185–201.
Gardner, R., Lookingbill, T., Townsend, P., Ferrari, J., 2008. A new approach for rescaling land cover data. Landscape Ecol. 23, 513–526.
Hulshoff, R., 1995. Landscape indices describing a Dutch landscape. Landscape Ecol. 10, 101–111.
Jaeger, J., 2000. Landscape division, splitting index, and effective mesh size: new measures of landscape fragmentation. Landscape Ecol. 15, 115–130.
Kasetkasem, T., Arora, M., Varshney, P., 2005. Super-resolution land cover mapping using a Markov random field based approach. Remote Sens. Environ. 96, 302–314.
Keshava, N., Mustard, J., 2002. Spectral unmixing. IEEE Signal Proc. Mag. 19, 44–57.
Langford, W., Gergel, S., Dietterich, T., Cohen, W., 2006. Map misclassification can cause large errors in landscape pattern indices: examples from habitat fragmentation. Ecosystems 9, 474–488.
Lausch, A., Herzog, F., 2002. Applicability of landscape metrics for the monitoring of landscape change: issues of scale, resolution and interpretability. Ecol. Indicators 2, 3–15.
Li, H., Wu, J., 2004. Use and misuse of landscape indices. Landscape Ecol. 19, 389–399.
Ling, F., Xiao, F., Du, Y., Xue, H., Ren, X., 2008. Waterline mapping at the subpixel scale from remote sensing imagery with high-resolution digital elevation models. Int. J. Remote Sens. 29, 1809–1815.
Makido, Y., Shortridge, A., Messina, J., 2007. Assessing alternatives for modeling the spatial distribution of multiple land-cover classes at sub-pixel scales. Photogramm. Eng. Remote Sens. 73, 935–943.
McGarigal, K., Cushman, S.A., Neel, M.C., Ene, E., 2002. FRAGSTATS: spatial pattern analysis program for categorical maps. Computer software program produced by the authors at the University of Massachusetts, Amherst. Available from: www.umass.edu/landeco/research/fragstats/fragstats.html.
Mertens, K., Verbeke, L., Ducheyne, E., De Wulf, R., 2003. Using genetic algorithms in sub-pixel mapping. Int. J. Remote Sens. 24, 4241–4247.
O'neill, R., Hunsaker, C., Timmins, S., Jackson, B., Jones, K., Riitters, K., Wickham, J., 1996. Scale problems in reporting landscape pattern at the regional scale. Landscape Ecol. 11, 169–180.
Peng, J., Wang, Y., Zhang, Y., Wu, J., Li, W., Li, Y., 2010. Evaluating the effectiveness of landscape metrics in quantifying spatial patterns. Ecol. Indicators 10, 217–223.
Purtauf, T., Thies, C., Ekschmitt, K., Wolters, V., Dauber, J., 2005. Scaling properties of multivariate landscape structure. Ecol. Indicators 5, 295–304.
Saura, S., 2004. Effects of remote sensor spatial resolution and data aggregation on selected fragmentation indices. Landscape Ecol. 19, 197–209.
Saura, S., Castro, S., 2007. Scaling functions for landscape pattern metrics derived from remotely sensed data: are their subpixel estimates really accurate? ISPRS J. Photogramm. Remote Sens. 62, 201–216.
Saura, S., Martínez-Millán, J., 2000. Landscape patterns simulation with a modified random clusters method. Landscape Ecol. 15, 661–678.
Schindler, S., Poirazidis, K., Wrbka, T., 2008. Towards a core set of landscape metrics for biodiversity assessments: a case study from Dadia National Park, Greece. Ecol. Indicators 8, 502–514.
Shao, G., Wu, J., 2008. On the accuracy of landscape pattern analysis using remote sensing data. Landscape Ecol. 23, 505–511.
Shen, W., Darrel Jenerette, G., Wu, J., Gardner, H.R., 2004. Evaluating empirical scaling relations of pattern metrics with simulated landscapes. Ecography 27, 459–469.
Tatem, A., Lewis, H., Atkinson, P., Nixon, M., 2001. Super-resolution target identification from remotely sensed imagesusing a Hopfield neural network. IEEE Trans. Geosci. Remote 39, 781–796.
Tatem, A., Lewis, H., Atkinson, P., Nixon, M., 2002. Super-resolution land cover pattern prediction using a Hopfield neural network. Remote Sens. Environ. 79, 1–14.
Tolpekin, V., Stein, A., 2009. Quantification of the effects of land-cover-class spectral separability on the accuracy of markov-random-field-based superresolution mapping. IEEE Trans. Geosci. Remote 47, 3283–3297.
Turner, M., 1990. Spatial and temporal analysis of landscape patterns. Landscape Ecol. 4, 21–30.
Uuemaa, E., Roosaare, J., Mander, Ü., 2005. Scale dependence of landscape metrics and their indicatory value for nutrient and organic matter losses from catchments. Ecol. Indicators 5, 350–369.
Verhoeye, J., De Wulf, R., 2002. Land cover mapping at sub-pixel scales using linear optimization techniques. Remote Sens. Environ. 79, 96–104.
Wu, J., 2004. Effects of changing scale on landscape pattern analysis: scaling relations. Landscape Ecol. 19, 125–138.
Wu, J., Shen, W., Sun, W., Tueller, P., 2002. Empirical patterns of the effects of changing scale on landscape metrics. Landscape Ecol. 17, 761–782.
Zheng, D., Heath, L., Ducey, M., 2008. Modeling grain-size dependent bias in estimating forest area: a regional application. Landscape Ecol. 23, 1119–1132.